STM JOURNALS

Journal of
Geotechnical Engineering

ISSN: 2394-1987
Volume 12, Issue 3, 2025
September–December
DOI (Journal): 10.37591/JoGE

https://journals.stmjournals.com/joge

Research JoGE

Comparative Analysis of Pond Ash as a Partial Replacement of Sand as Subbase Material for Concrete Paver Block Hardstand Sustaining Storage of Bulk Cargo

Aditya Shankar Ghosh[1,*], Nepal Chandra Porey[2], Priti Rajak[3], Rabindranath Mal[4], Ranjan Kumar[5], Raju Ranjan Kumar[6], Rinki Roy[7], Tapash Kumar Roy[8]

Abstract

This work presents an industrial waste-derived subbase material that can take the place of conventional granular material for subbase in hardstand foundation construction. This industrial waste hugely deposited in the ash lagoons namely Pond Ash (PA) which is globally generated at an amount of 780 Metric Tons from thermal power plants annually ,as foundation material for hardstand construction, will not only help the cause of residual waste disposal problems but will also solve other associated shortcomings like, lower utility and degrading environmental impact, and will also provide an economic alternative. This study analyses the geotechnical, morphological, mineralogical and polymeric properties of PA samples, designs a numerical model for safe foundation depth and a physical model for measuring the deflection using Light Falling Weight Deflectometer (LFWD) using PA as subbase material, replacing Sand as CGM along with the associated cost benefit. The research work reveals that PA in itself be a suitable material for foundation subbase. The LFWD shows peak surface deflection modulus differs only by 1% from CGM.

Keywords: Pond ash, chemical composition, geotechnical and polymeric characteristics, XRD, FTIR, microstructure, light falling weight deflectometer

INTRODUCTION

The disposal of waste products and by-products is one of the biggest issues facing processing and manufacturing industries. These readily available residual wastes are directly associated with the production of electricity by the combustion of coal, which results in the deposition of ash at the bottom in major quantities identified as Bottom Ash (BA), which is subsequently combined with water and kept in ash lagoons to create Pond Ash (PA). Indian coal-based thermal power plants generate 221 MT of PA annually, which is the highest [1–25]. Continuity of this and fuelled by India's vast coal reserve, it is estimated that 600 MT of PA will be generated annually by the year 2031-2032. However, with the current level of PA utilization efforts in India reaching nowhere near its 100% utilization target [8], its availability is becoming more appreciated. In contrast, condemning the use of sand became necessary owing to the rising consumption of aggregates in concretization, including its burial in foundation layers [1–11]. Under such conditions, the need for affordable building materials with fewer adverse effects on the environment is rapidly expanding. Therefore,

***Author For Correspondence**
Aditya Shankar Ghosh
E-mail: adityabesus2011@gmail.com

[1]Research Scholar, Department of Civil Engineering, Indian Institute of Engineering Science and Technology, Shibpur, West Bengal, India
[2-7]Undergraduate Student, Department of Civil Engineering, Dream Institute of Technology, Kolkata, India
[8] Associate Professor, Department of Civil Engineering, Indian Institute of Engineering Science and Technology, Shibpur, West Bengal, India

Received Date: July 10, 2025
Accepted Date: July 30, 2025
Published Date: August 03, 2025

Citation: Aditya Shankar Ghosh, Nepal Chandra Porey, Priti Rajak, Rabindranath Mal, Ranjan Kumar, Raju Ranjan Kumar, Rinki Roy, Tapash Kumar Roy. Comparative Analysis of Pond Ash as a Partial Replacement of Sand as Subbase Material for Concrete Paver Block Hardstand Sustaining Storage of Bulk Cargo. Journal of Geotechnical Engineering. 2025; 12(3): 32–45p.

because of its pozzolanic qualities, PA is considered as an alternative subbase material in this research. Much successful work has already been done using cement [26, 27] and lime [4] stabilized coal combustion ash along with fiber reinforcement [26, 28, 29] as a material for subbase construction for pavements; however, few attempts have been made to use virgin PA as a hardstand foundation subbase material where sand is generally used.

Therefore, this study attempts to provide methods for the dependable integration of virgin PA from ash disposal ponds into hardstand foundation layers. This study tested the geopolymeric nature of PA in an alkaline environment [30–35] and used laboratory test data to mathematically calculate the anticipated in situ behavior. By evaluating the deviation from the physical model, created using PA as a subbase material under LFWD, mathematical design charts are ultimately produced to help users determine the safe thickness of foundation layers, including PA.

Hardstand Foundation Layer Practice and Materials Used

In practice, the Hardstand foundation layer is similar to that of the conventional flexible pavement foundation layer [26, 31], mostly the subgrade, unbound, and bound layers, which are frequently completed before the surfacing course [17]. Locally available soil was used as the subgrade layer. The subbase is composed of unbound granular materials such as crushed stones, moorum, natural sand, and gravel [2]. Water Bound Macadam (WBM) or Wet Mix Macadam (WMM) forms an unbound base layer, where physical interlocking and suction due to water-added compaction between the materials hold them together. The bound layer is divided into Dense Bituminous Macadam over the WBM preceded by Bituminous Concrete (BC), Cement Concrete (CC) slab, or Concrete Block Pavement (CBP) [17].

Situation in India

India is ranked 16th in terms of its largest maritime country worldwide. Maritime transportation has been instrumental for 95% of the country's trading volume and 70% by valuation. The cargo traffic at major ports of the country increased by 2.41% from the financial year 2017 to 679.39 MT [9], and the Indian government has planned to develop six new strings of mega ports to provide further boost to the country's economy. This program has bought lakhs of square meters of area under the construction schedule forhardstand.

In contrast, Indian thermal power plants produced 217.04 MT of PA in 2018-19 [26] and utilized 168.40 MT of PA, suggesting an effective usage of 77.59% [8]. This high production and low percentage utilization of PA has already consumed an area of 65000 acres of land and is planned to occupy more as the PA generation is expected to cross 225 MT in the near future [27]. In addition to the consumption of acres of land, disposed PA cause serious environmental and health hazard [10]. However, the extensive construction schedule has led to increasing consumption of naturally occurring aggregates [8], making it necessary to formulate "The Sustainable Sand Mining Management Guideline 2016," which condemns the extensive use of sand in concretization, including its burial for foundation layers [8]. The main focus of this research is to discuss the possibility of virgin PA as a material for the confinement subbase layer in hardstand construction.

THE RATIONALE BEHIND REPLACING CGM BY POND ASH

This study goes through numerous investigations, suggesting plenty of successful case histories of the utilization of Coal Ash as a partial replacement. Investigators have used 9% cement and 3% FA to stabilize soil for pavement foundations [4], embankment construction materials [24], and structural fill [6]. Researchers have used it for grouting [15] and as a partial replacement of cement by up to 30% by weight [12] for subsidence control [20]. Research has indicated that the use of pulverized coal ash filler lowers the possibility of mining pillar failure and has been effectively used to stabilize it [7]. Coal ash mixed at 15% to 20% by weight along with mill tailings, rock, and binding agents has been found to be effective in making a consolidated backfill material that improves the extraction percentage in coal mines [23].

Studies on container port pavements have shown that coal ash is useful as an inexpensive, low-maintenance binder in hydraulically bound mixtures for base and sub-base courses [16]. The removal and replacement technique used in this study was previously undertaken by researchers, where unsuitable soils were replaced with marine fill sand [22], and Recycled Concrete Aggregate (RCA) was used for the base course [28].

Investigators have conducted extensive research on BA as a subbase material [1], along with the results from cyclic triaxial tests that have helped in understanding the resilient and plastic behavior of Coal Combustion Ash (CCA) [19]. The compacted aggregate-free, cement-stabilized CCA base at 10% by weight provided researchers with satisfactory performance for the base layer of pavements [13]. CCA mixed with additives such as gypsum and lime 15%-20% and 0%-5% by weight, respectively, is used for pavement foundation layers [21]. Polypropylene fibers are added to FA as admixtures in 0.5% by weight and utilized as fiber-reinforced CCA in road subbases [29]. Cement- and GBFS-stabilized FA mixes of 8% and 40% by weight, respectively, provided sufficient CBR for the mixture to be suitable for the base and subbase of roadway pavements [12, 30]. Geotechnical characterization of CCA composites was performed to backfill mine voids [21]. Experiments conducted to check the durability and strength of lime-stabilized FA provided satisfactory results such that they could find applications in the base and subbase course of pavements [3], and satisfactory investigational works were also conducted on the resilient characteristics of BA [32]. Pavements with a cement-treated base layer, with and without FA, showed a comparatively more suitable performance [18]. Studies have revealed that the physical, chemical, morphological, and mineralogical analysis of CCA, along with its mechanical performance and polymeric properties [35], compares favorably with CGM and can be effectively used as an economic highway material [14].

In 1970, geopolymers were conceptualized as inorganic cementitious materials, primarily composed of an excessive percentage of silicon aluminum natural minerals, mainly in solid waste [36]. These are formed by the polymerization of inorganic polymers. CCA, which has this required chemical composition, has been used by researchers to successfully prepare mineral polymeric materials [37, 38]. Recently, many studies have been conducted by considering the impact of CCA-based polymer materials and the broad prospects of their applications [39–41].

The literature reviews showed successful outcomes because FA can be utilized as a replacement material for the unbound base and subbase layers of pavements using different additives [11]. However, there is a lacuna in the behavior of hardstand foundation layers using virgin PA without any additives or reinforcements as the sub-base layer material. Restrictions on extensive sand usage have made it necessary to utilize PA as a hardstand sub-base layer material. In addition to its hydrophobic quality, which increases its capacity to absorb and release water and strengthens its permeability, its pozzolanic nature along with its geopolymeric attributes guarantees the stability of the subbase layer [8]. Another associated challenge is determining the safe depth of the newly formed subbase layer, which is important for the construction cost and corresponding service life of the structure.

AIM AND SCOPE OF WORK

This investigation is aimed at the utilization of virgin PA as a subbase material in the confinement of a hardstand foundation, and provides it with a safe depth, which will allow adequate structural performance, which is also economical. The experiment was carried out in two stages to understand the behavior of the virgin PA without any additives. The purpose of this study was to evaluate the strength, deformability, volume stability, permeability, and erodibility of virgin PA samples in comparison to CGM, which is to be used as a replacement for CGM for confined subbase layer construction of hardstand foundations. Comparative analysis was performed between the CGM and virgin PA samples to determine their suitability for application by performing proctor compaction, triaxial tests, Unconfined Compressive Strength (UCS) tests, etc. Important geotechnical properties were analyzed and used in this study for numerical analysis of the safe subbase layer depth calculation.

The Mineralogical, morphological, and polymeric characteristics of the PA samples were analyzed to determine their suitability as subbase layer materials. This was followed by the preparation of a physical model to evaluate the performance of the compacted samples using LFWD. The test data were analyzed using LWDmod software to obtain the differences in the Peak Surface Deflection Modulus (E_{SURF}) and corresponding Peak Surface Deflection for the samples.

METHODOLOGY AND EXPERIMENTAL PROGRAM

The experiment was performed in two stages: characterization of the collected PA sample, evaluation of the geotechnical properties, and calculation of the safe foundation layer depth using standard mathematical calculations. The chemical properties of the samples were analyzed in the IIEST Shibpur chemistry laboratory, followed by an analysis of the geotechnical properties that were performed in the geotechnical laboratory of the same. The outcomes were validated by analyzing the morphological, mineralogical, and polymeric properties of the sample obtained from the Metallurgy Department, Centre of Excellence in Green Energy and Sensor (CEGESS) IIEST, Shibpur, and S.N. Bose National Centre for Basic Sciences (SNBCBS).

Collection of Pond Ash

PA was obtained from a Kolaghat Thermal Power Station ash pond in West Bengal, China. PA is a pozzolanic material, and the purpose of using it as a replacement for sand in this research work is mainly based on this property, which further conforms to the requirements given in Tables 1 and 2 of MORT&H. This improves the strength, deformability, and permeability durability of the foundation layers to be used.

Table 1. Chemical compositions of PA.

Chemical constituents	Percentage
Silica (SiO_2)	77.50%
Alumina (Al_2O_3)	1.07%
Magnesium Oxide (MgO)	1.30%
Iron (II) Oxide (Fe_2O_3)	12.65%
Calcium Oxide (CaO)	2.65%
Loss on Ignition	1.05%
Others	3.78%

Table 2. Geotechnical properties of PA.

Geotechnical properties	Corresponding values
Fine sand size 0.475 – 0.075 mm (%)	46.1
Silt size 0.075 – 0.002 mm (%)	53.8
Uniformity Coefficient (C_u)	1.306
Coefficient of curvature (C_c)	0.867
Effective Size (D_{10}) mm	0.062
D_{30} size mm	0.066
D_{60} size mm	0.081
Specific Gravity	2.103
Liquid Limit and Plastic Limit	Non-plastic
Maximum dry unit weight kN/m3	11.8
Optimum Moisture Content (OMC) (%)	25.86
Permeability (cm/sec)	0.000157
Properties obtained from Triaxial Test	
Bulk Density g/cc	1.49
Cohesion Intercept (c) kg/cm^2	0.88
Angle of shearing resistance (φ^o)	32

Chemical and Geotechnical Properties of Virgin Pond Ash

Tables 1 and 2 show the chemical composition and geotechnical properties of the PA sample, respectively.

Mineralogical Composition of Virgin Along with 7, 14 and 28 Days Hydrated Pond Ash

Mineralogical characterization of the PA sample aids in determining its composition. It also sheds light on the mineral phases present in the sample along with the structural characterization of the polymeric material [35]. The diffractograms of X-Ray Diffraction (XRD) followed by Fourier Transform Infrared (FTIR) spectroscopy helped in further determination of the undetected phases present.

Preparation and Characterization (XRD and FTIR) of Sample

Mineralogical tests were performed on the virgin sample and the sample with water added according to its OMC and kept at room temperature for 7, 14, and 28 days to check the development of the pozzolanic phase.

A ULTIMA IV X-RAY DIFFRACTOMETER automated with Cu-Kα radiation was used for XRD.The, and the PA samples for FTIR were prepared in the same manner as the XRD. They were pressed into KBr pellets using Nicolet 7199 FT-IR. FTIR provided a good understanding of the average chemical structure of the samples at various stages of the PA hydration process.

Morphological Characterization (FESEM, EDS and AFM) of Virgin Pond Ash Sample

The morphological characterization and compositional information of the PA sample in this study were accumulated using Field Emission Scanning Electron Microscopy (FESEM), Energy Dispersive X-ray Spectroscopy (EDS), and Atomic Force Microscopy (AFM).

FESEM analysis of the PA sample was performed using a JEOL-JSM-7610F. The dried powdered PA sample was placed on a specimen holder plate attached to a double-layer carbon adhesive. This plate was transferred to a sputter coater (POLARAN E 5100), and a thin conducting layer of platinum was deposited on the specimen surface [5]. Electron images of the surface morphology were taken at 100μm to 10 μm magnification.

EDS was performed on electron images taken at 500 μm and 50 μm magnification was carried out to determine the chemical elements present in the PA sample.

AFM allows imaging of the sample surface without any special preparation. The surface topography of the PA sample was analyzed using DI-INNOVA 840-012-706 AFM. The tapping Mode or Intermediate Contact Mode was selected at a resonating frequency of 300 kHz and amplitude of 60 Å using a 10 μm scanner [5].

Light Falling Weight Deflectometer

The LFWD used in this study was DYNATEST 3031 LWD to determine the modulus and compaction of the samples. The diameter of the loading plate is 300 mm. The measured deflection at the center of the plate was used to calculate the dynamic deformation modulus (E_{LFWD}) using the Boussinesq solution, as follows:

$$E_{LFWD} = \frac{k(1-\nu^2)\sigma R}{\delta_c}$$

where $k = \pi/2$or 2 for rigid and flexible plates, respectively. δ_c = center deflection, σ = applied stress, and R = radius of the plate.

Preparation and Testing of Samples

A cast iron mold with a diameter of 360 mm and a depth of 650 mm was used to test the compacted layers. A 0.50 m subgrade clay layer was first compacted at the OMC topped by the base layer compacted into a 0.11 m thick lift. The desired water content was achieved by drying the samples in an

oven. Then, the PA was hand mixed homogeneously with the desired amount of water and compacted within the mold. A freeboard (0.04 m was left for the proper functioning of the equipment. Compaction was performed using a modified proctor and left for 72 h for further settlement. The compaction energy equivalent was measured to determine the number of blows per layer in the test mold.

RESULTS AND DISCUSSIONS

The results obtained from the experimental programs are discussed below:

X-Ray Diffraction (XRD) Analysis

The XRD pattern showed the predominant presence of crystalline Mullite, Silicon Oxide and Silicon Phosphate. Silica is present partly in the crystalline form of Silimanite and Quartz, in addition to alumina as mullite. Iron appears as an oxide of magnetite and, minutely, as hematite. Figure 1 shows the peaks of Calcium Hydroxide at 18.7° and Calcium Carbonate at 42.6° [8], revealing the pozzolanic nature of PA.

Fourier Transform Infrared (FTIR) Spectroscopy

The FTIR spectra in Figure 2 show absorbance at 3440 cm$_{-1}$ and 1650 cm$_{-1}$ due to the water and silanol groups, respectively. It is related to the free water adsorbed on the surface of the mineral polymer precursor [42]. In the precursor of mineral polymeric materials, the anti-symmetric stretching vibration absorption peak of C-H is located at 2,963 cm^{-1}, whereas the peak near 806 cm^{-1} might represent the unreacted Si-OH bending vibration absorption peak (Guo, 2016). According to infrared spectroscopic investigation, the peak value of Si-OH increases as the dose of ethanol increases, and this has a major impact on the absorption peak of the mineral polymer precursor [43]. The wide peak at approximately 1080 cm^{-1} represents siloxanes that transform into aluminum silicate bonds of poly-Sialate at approximately 910 cm^{-1}. Quartz was observed at 1160 cm^{-1} [34]. This provides a binding nature to PA, thus providing a certain stability.

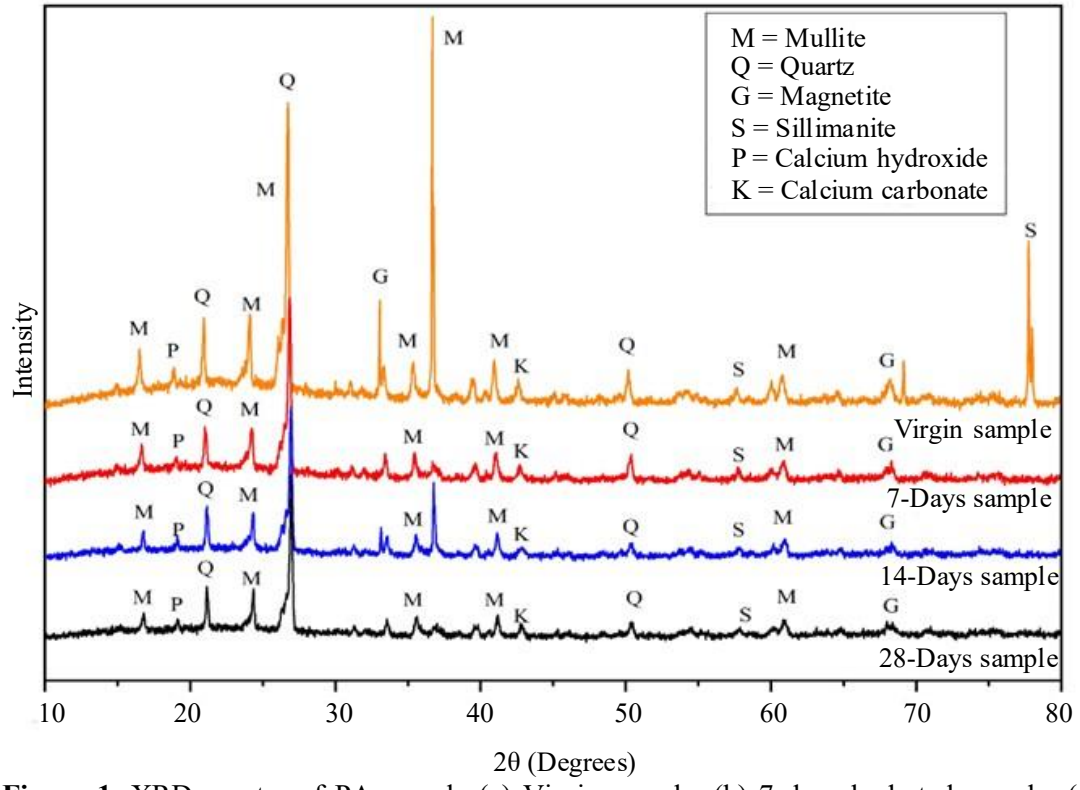

Figure 1. XRD spectra of PA sample (a) Virgin sample, (b) 7 days hydrated sample, (c) 14 days hydrated sample, and (d) 28 days hydrated sample.

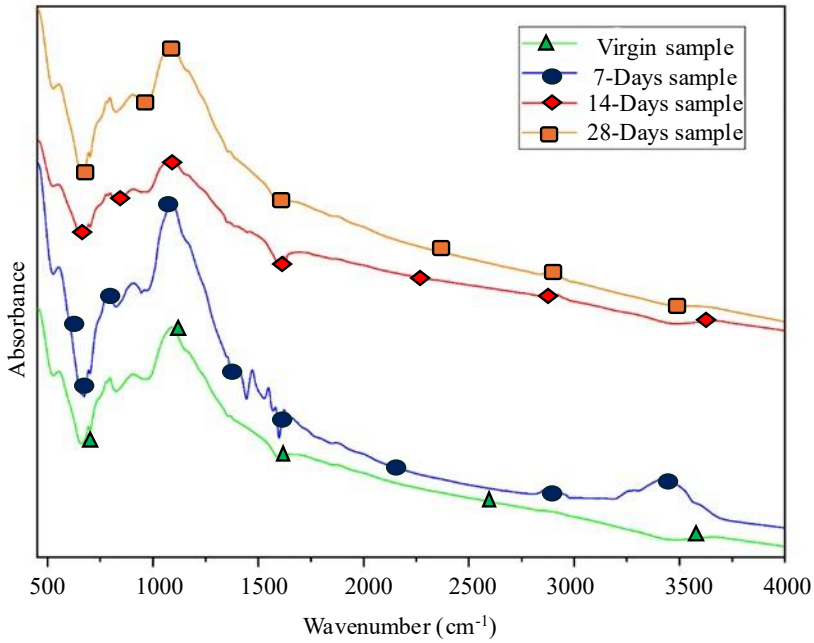

Figure 2. Quantitative FTIR analysis of PA sample (a) Virgin Sample, (b) 7 days hydrated sample, (c) 14 days hydrated sample, and (d) 28 days hydrated sample.

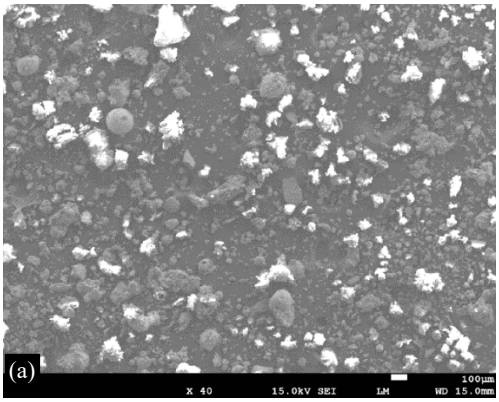

Figure 3. (a) FESEM image of the PA sample at 100µm magnification showing the presence of some clustered particles.

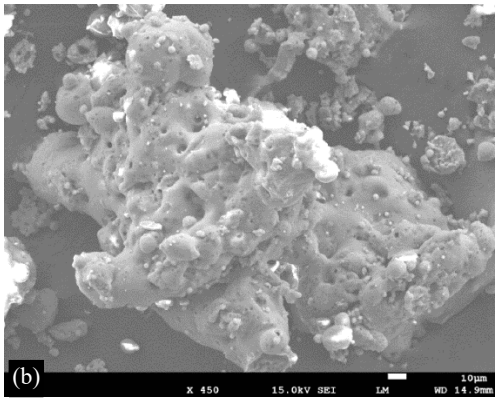

Figure 3. (b) FESEM image of the PA sample at 10µm magnification showing the presence of multi-layered porous structure of the particles.

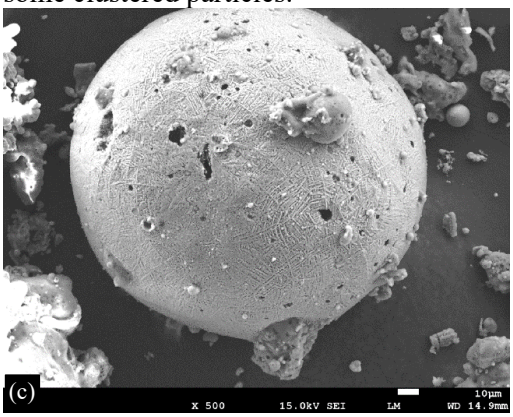

Figure 3. (c) FESEM image with 10µm magnification zooming on one of the clustered particle in the PA sample showing the surface morphology of the particles.

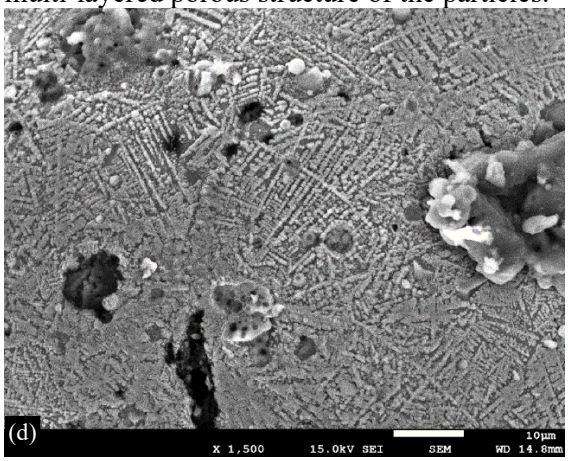

Figure 3. (d) Zooming (1µm) on the particle surface.

Field Emission Scanning Electron Microscopy (FESEM)

Microstructural analysis of the PA sample using FESEM revealed that it contained particles of different diameters and compositions. Figure 3(a) shows the partial inertness of these particles. However, enlarged clusters of porous particles amalgamated with other particles are also visible in Figure 3c, indicating their pozzolanic properties. Figure 3(b) shows images zoomed into the surface texture of the particles fused together, with hollow cavities in the clusters that tend to absorb more water. This explains the porosity and hygroscopicity of the samples. The higher-magnification images in Figure 3(c) show cluster formation, although very little, with an almost spherical shape. However, magnifying the image in Figure 3(d) represents the net formation already taking place, imparting cohesiveness and stability to the sample.

Energy Dispersive X-Ray Spectroscopy (EDS)

EDS (Figure 4) showed the presence of O and Ca, along with significant levels of C, Al, Si, Mg, Na, and Fe, which supported the data obtained from the chemical analysis of the sample and trace amounts of Mn, Ti, Cu, and Zr.

Atomic Force Microscopy (AFM)

Figure 5(a-b) shows an AFM image of the PA sample surface emerging above the adhesive. The image taken at the 10µm scan shown in Figure 5(a) represents the overall topography of the PA sample surface. Figure 5(b) shows the presence of particle clusters formed owing to the pozzolanic nature of the sample. The round, crater-like dark areas indicate the porosity of the sample. The images were acquired in the intermittent mode; therefore, poorly adhering surface particles remained undisturbed. Figure 5(c) shows the uneven topography of the sample, which provided surface friction and cohesiveness. Figure 5(d) shows the layered nature of the surface, revealing the reactivity of the PA sample [5].

Light Falling Weight Deflectometer

The LFWD measurements were collected in 3031 LWD 5.1, and the analysis of the data was performed using Dynatest LWDMOD, which lists the stress generated, deflections produced, and surface deflection moduli obtained for all 15 drops of the drop weight executed on the PA and sand layers inside the mold. The graphical representation Figure 6 of the surface deflection and surface deflection modulus for the PA and sand showed minimal alteration. The average surface deflection moduli for PA and sand were 20.133 MPa and 19.933 MPa, respectively. The cohesive nature of PA is instrumental for developing this interparticular bonding, thus providing minimalistic deflection under the impact of the load.

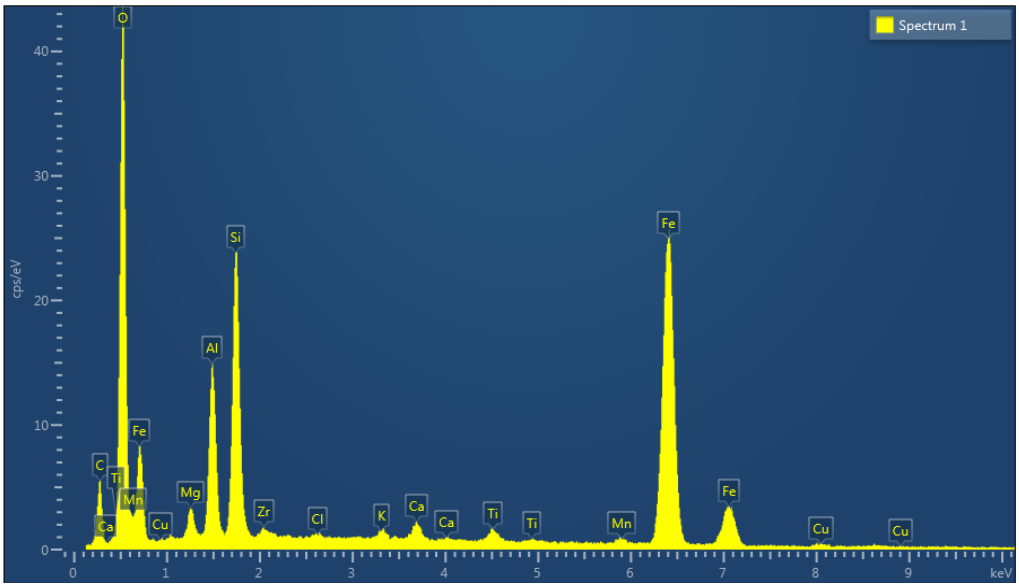

Figure 4. Energy dispersive spectroscopy spectrum of the mineral crust of the PA sample.

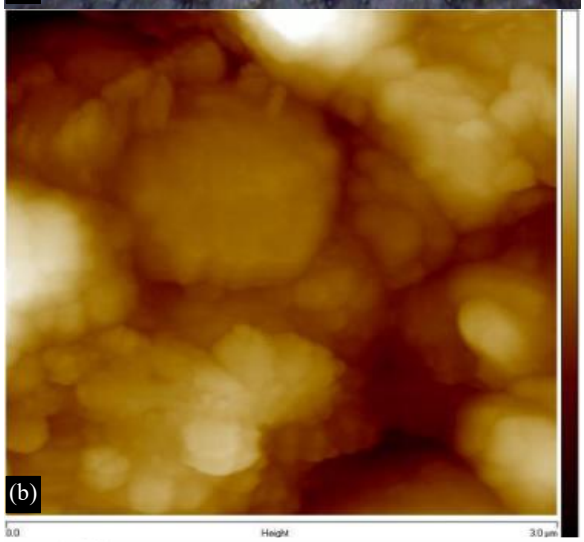

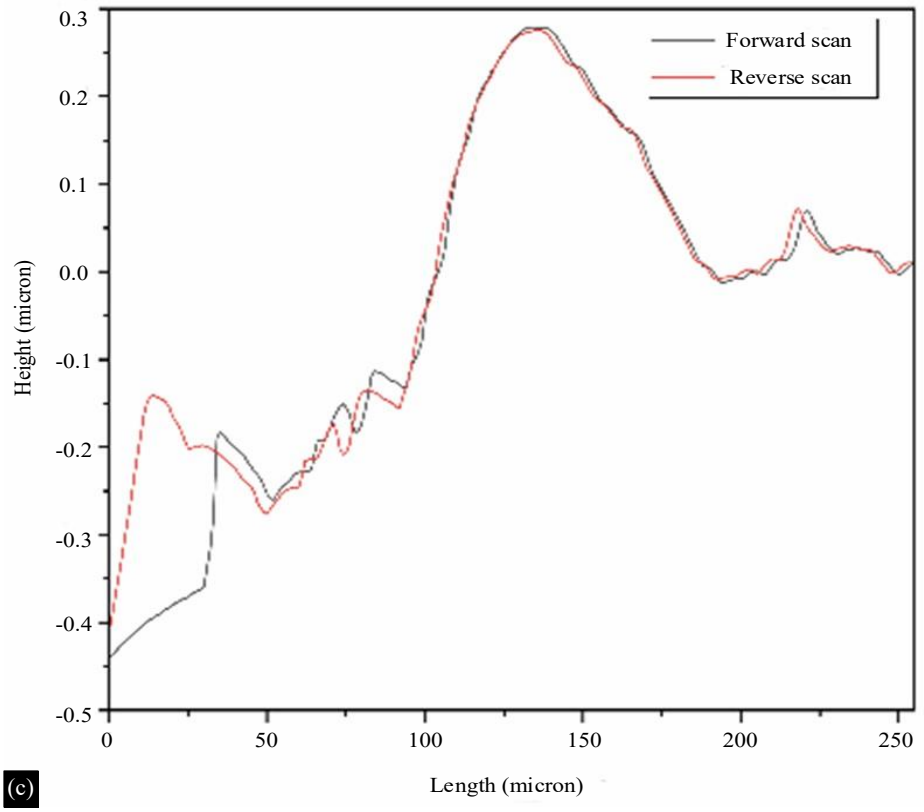

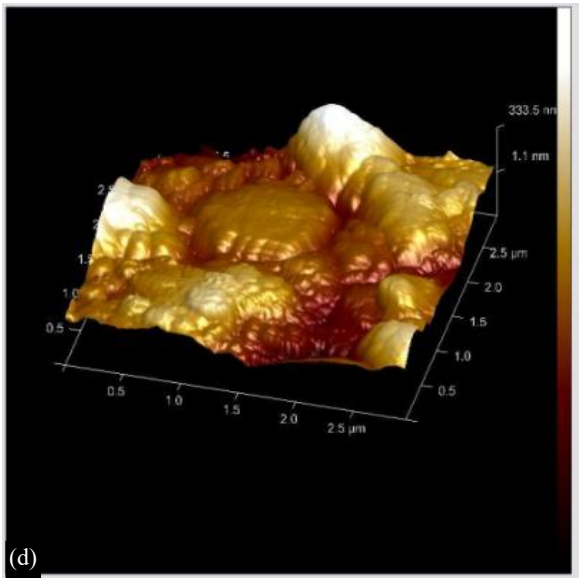

Figure 5. (a) Surface morphology of the pond ash, (b) Particle Cluster formation along with its porous and layered structure, (c) Height Profile of craters on the surface of the pond ash, (d) Surface topography of the pond ash sample.

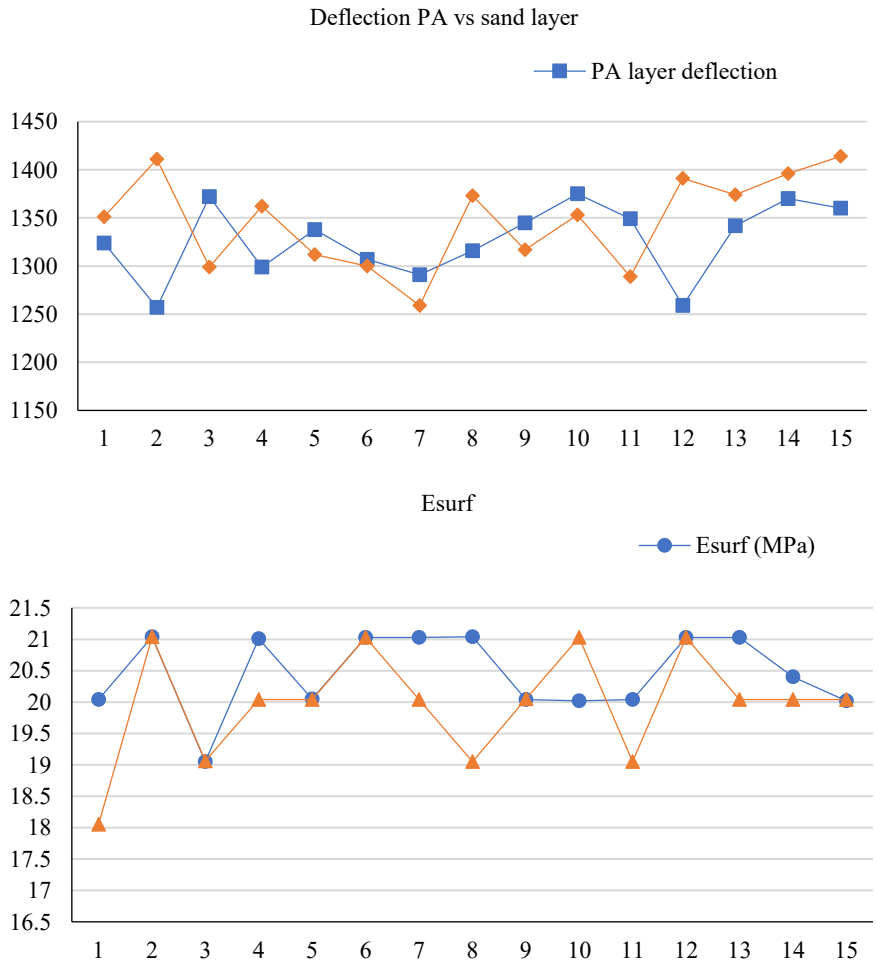

Figure 6. Graphical representation of the comparative analysis of deflection and surface deflection moduli (E_{surf}) for PA and sand zone (III) under the application of LFWD.

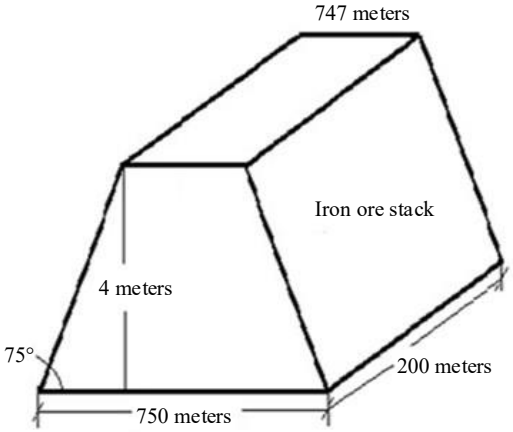

Figure 7. Schematic diagram of the proposed iron ore stack.

DESIGN SPECIFICATIONS

The design specifications for the foundation presented in this paper are for a rectangular footing with a planned area of 750 m x 200 m, carrying iron ore stacked up 4mtr a height, having specific gravity ranging from 4.5-5.3. The foundation was placed at a depth of 1.5mtr below ground level. The safe depth of the foundation was evaluated using [33] for the design of a shallow foundation using cohesionless soil. The footing was subjected to a load inclined at 15° in the vertical direction, as shown in Figure 6. The geotechnical properties of the PA sample used for this purpose were evaluated, including the saturated unit weight and the C and φ values (Table 2). The magnitude of the load to be carried by the footing is calculated assuming the rate of loading to be such that drained conditions prevail.

DESIGN SPECIFICATIONS

The design of the foundation for this study is based on the ultimate bearing capacity and limiting settlement for a footing on cohesionless soil with a drained loading problem. The predicted bearing capacity is estimated considering the PA sample to be used as the foundation layer material by the theory proposed by (Vesic1973) in the following equation:

$$q_{nd} = cN_c s_c d_c i_c + q\left(N_q - 1\right)s_q d_q i_q + \frac{1}{2}B\gamma N_\gamma s_\gamma d_\gamma i_\gamma w'. \quad (1)$$

where c is the unit cohesion, q_{nd}= bearing capacity, q = effective overburden pressure, B is the footing width, γ = the effective unit weight of the PA sample, w'= the moisture content. The model in Eqn. (1) has evolved over the years and has been researched extensively.

The effective overburden pressure is evaluated using a trial and error method by changing the depth of the foundation using the following equation:

$$q = D_f \times \gamma \quad (2)$$

where D_f =Depth of the foundation.

The factors used in the eqn.1 are N_c, N_q, N_γ = Bearing capacity factors; s_c,s_q,s_γ= shape factors; d_c,d_q,d_γ= depth factors; and i_c,i_q,i_γ= inclination factors as per the proposition of Vesic [33].

The calculation of the safe load is done by

$$(q_{net})safe = \frac{q_{nd}}{Fs} \quad (3)$$

where Fs = Safety factor.

The measured safe load was compared with the vertical load acting on the rectangular foundation shown in Figure 7 and was found to be safe for a foundation depth of 1.5 meter. Table 3 lists the variation in the measured load with respect to the considered foundation depth.

Table 3. Chemical compositions of pond ash.

S.N.	Vertical load	Foundation depth	Measured load	Remarks
1.	4.50×10^7 Tonnes	1.3 meters	4.28×10^7 Tonnes	Unsafe
2.		1.4 meters	4.36×10^7 Tonnes	Unsafe
3.		1.5 meters	4.52×10^7 Tonnes	Safe

CONCLUSIONS

In this study, the chemical, geotechnical, morphological, and mineralogical properties of the Haldia PA sample were evaluated. Observations were made utilizing it as an alternate foundation material as a substitute for zone III sand for the construction of a foundation in a stackyard. The probable foundation depth of the PA sample was measured using Vesic's theory [33] for a shallow foundation using cohesionless materials. This was followed by a cost analysis comparing the costs of using both materials. The conclusions are as follows.

- The chemical composition of the sample revealed a higher percentage of SiO_2 and lower percentages of Al_2O_3, MgO, Fe_2O_3 and CaO. This is further supported by the EDS chemical analysis showing the presence of C, Al, Si, Mg, Na, and Fe in significant amounts along with O and Ca. indicating the pozzolanic properties of the sample. Traces of Mn, Ti, Cu, and Zr are also present.
- The geotechnical properties of the PA sample showed a certain cohesive nature along with the friction angle, providing stability in the absence of any additional agents suitable for its use as a foundation material. The hydraulic conductivity data also satisfactorily confirmed its validity as a foundation material.
- The XRD results showed the presence of Mullite, Quartz, Magnetite, Sillimanite, Calcium Hydroxide and Calcium Carbonate, confirming PA's pozzolanic property of PA. Iron appears as an oxide of magnetite and, minutely, as hematite. These peaks show the pozzolanic property, which imparts little cohesiveness and stability to the sample.
- FTIR Spectroscopy analysis revealed that the absorbance pattern was formed in the presence of water and silanol groups. The transformation of the Si-O-Si bonds of amorphous silica into the Si-O-Al bond of poly-Sialate is also conferred by this analysis, which specifies that the wavenumbers and absorbance values are due to the pozzolanic nature of the sample.
- The FESEM images of the PA sample showed that their surface texture fused with some hollow cavities, explaining the porous and hygroscopic nature of the sample. The images also reveal the layered structure, indicating the high reactivity of the sample, with some clear signs of net structure formation.
- The topography of the PA sample deduced by AFM displayed an interesting surface covered with craters and crests, reflecting the reactivity of the sample. The undulated topography provides the sample with surface friction and results in minimal cohesiveness and stability. The particles embedded in the surface were microcrystals of mullite, hematite, and magnetite, which were also obtained by XRD.
- The LFWD yielded measurements to measure the deflection caused by the PA and Zone III sand. The results suggest that PA can be effectively used as an alternate foundation material owing to its minimal deflection under the action of LFWD.

REFERENCES

1. Bullen F, Dawson AR. Furnace bottom ash: Its engineering properties and its use as a sub-base material. ICE Proc. 1991;90:993–1009.
2. Chakroborty P, Das A. Principles of Transportation Engineering. New Delhi: Prentice Hall of India; 2003.
3. Chand SK, Subbarao C. Strength and slake durability of lime stabilized pond ash. J Mater Civ Eng. 2007;19:601–8. doi:10.1061/(ASCE)0899-1561(2007)19:7(601).
4. Chu TY, et al. Soil stabilization with lime–fly ash mixtures: preliminary studies with silty and clayey soils. Highway Research Board Bull. 1995;108:102–12.

5. Demanet CM. Atomic force microscopy determination of the topography of fly-ash particles. Appl Surf Sci. 1995;89:97–101. doi:10.1016/0169-4332(95)00030-5.
6. DiGioia AM, Nuzzo WL. Fly ash as structural fill. J Power Div. 1972;98:77–92. doi:10.1061/JPWEAM.0000712.
7. Fawconnier CJ, Korsten RWO. Ash fill in pillar design – increased underground extraction of coal. SAIMM Monograph Ser. 1982;4:277–361.
8. Ghosh AS, Roy TK. Evaluating the utility of pond ash as an alternative foundation material partially replacing sand for foundation layers. In: Dey AK, Mandal JJ, Manna B, editors. Proc 7th Indian Young Geotechnical Engineers Conf. Singapore: Springer Nature; 2022. p. 157–65. doi:10.1007/978-981-16-6456-4_18.
9. Shankar Ghosh A, Roy A, Roy TK. Performance evaluation of nano-material stabilized pond ash as subbase layer material for roadway pavement. Mater Today Proc. 2023. doi:10.1016/j.matpr.2023.03.710.
10. Ghosh AS, Roy TK. Elemental assessment of pond ash for evaluating its application as a subbase material for hardstand construction. In: Muthukkumaran K, Jakka RS, Parthasarathy CR, Soundara B, editors. Soil Behavior and Characterization of Geomaterials. Vol. 296. Singapore: Springer; 2023. p. 99–114. doi:10.1007/978-981-19-6513-5_9.
11. Ghosh AS, Roy TK. Evaluating the durability of stabilized conventional granular material with pond ash and lime used as subbase course of flexible pavement. Mater Today Proc. 2022;65:1799–804. doi:10.1016/j.matpr.2022.04.821.
12. Gopalan MK, Haque MN. Strength development of chemically cured plain fly ash concretes. Proc Aust Road Res Board. 1986;13:27–33.
13. Gray DH, Tons E, Thiruvengadam TR. Performance evaluation of a cement-stabilized fly ash base. Transp Res Rec. 1994;1440:51–9.
14. Huang YH. Pavement Analysis and Design. Englewood Cliffs: Prentice Hall; 1993.
15. Joshi RC, Natt GS, Wright PJ. Soil improvement by lime–fly ash slurry injection. In: Proc 10th Int Conf Soil Mechanics & Foundation Engineering. Vol. 3. Stockholm; 1981. p. 707–12. https://www.issmge.org/publications/publication/soil-improvement-by-lime-fly-ash-slurry-injection
16. Knapton J. The Structural Design of Heavy Duty Pavements for Ports and Other Industries. Leicester: Interpave; 2007.
17. Knapton J, Barber SD. The behaviour of a concrete block pavement. Proc Inst Civ Eng Transp. 1979;66:277–92.
18. Ksaibati K, Conklin TL. Field performance evaluation of cement-treated bases with and without fly ash. Transp Res Rec. 1994;1440:16–21.
19. Lee SW, Fishman KL. Resilient and plastic behaviour of classifier tailings and fly ash mixtures. Transp Res Rec. 1993;1418:8–15.
20. Maser KR, Wallhagen RE, Dieckman J. Development of fly ash cement mine sealing system. USBM Open File Rep. 1975;26–76. NTIS-PB-250611.
21. Mishra MK, Karanam UMR. Geotechnical characterization of fly ash composites for backfilling mine voids. Geotech Geol Eng. 2006;24:1749–65. doi:10.1007/s10706-006-6805-8.
22. Ospina CE, Kumar VK, Puente J. Design of container yard at Port of Balboa. 2010. https://trid.trb.org/View/927149
23. Palariski J. The use of fly ash tailings, rocks and binding agents as consolidated backfill for coal mines. In: Proc Mine Fill. SAIMM; 1993. p. 403–8.
24. Raymon S. Pulverized fuel ash as embankment material. Proc Inst Civ Eng. 1961;19:515–36. doi:10.1680/iicep.1961.11308.
25. Sahu SK, Bhangare RC, Ajmal PY, Sharma S, Pandit GG, Puranil VD. Characterization and quantification of persistent organic pollutants in fly ash from coal-fuelled thermal power stations in India. Microchem J. 2009;92:92–6.
26. Sarkar R, Dawson AR. Economic assessment of use of pond ash in pavements. Int J Pavement Eng. 2017;18:578–94. doi:10.1080/10298436.2015.1095915.

27. Sarkar R, Abbas SM, Shahu JT. A comparative study of geotechnical behaviour of lime stabilized pond ashes from Delhi region. Int J GEOMATE. 2012;3(1):273–9.
28. Sieglen WE, Langsdorff HV. Interlocking concrete block pavements at Howland Hook marine terminal. Ports Conference, Houston, Texas, United States; 2004.
29. Singh SP, Kumar P. Utilization of fibre reinforced fly ash in road sub-bases. In: Fly Ash Utilization Programme (FAUP). TIFAC, DST; 2005. Vol VIII. p. 17.1–8.
30. Singh SP, Ramaswamy SV. Utilization potential of cement stabilized flyash–GBFS mixes in highway construction. Fly Ash Utilization Programme (FAUP). TIFAC, DST; 2005. Vol VIII. p. 4.36–14.11.
31. Thoresen CA. Port Designer's Handbook. London: Thomas Telford Publishing; 2003.
32. Titi HH, Coenen AR, Elias MB. Resilient characteristics of bottom ash. In: Tutumluer E, Al-Qadi IL, editors. Bearing Capacity of Roads, Railways and Airfields. Taylor & Francis Group; 2009. p. 117–24. ISBN: 978-0415-87199-0.
33. Vesic AS. Analysis of ultimate loads of shallow foundations. Int J Rock Mech Min Sci Geomech Abstr. 1974;11:A230. doi:10.1016/0148-9062(74)90598-1.
34. Rees CA, Provis JL, Lukey GC, Van Deventer JSJ. Attenuated total reflectance Fourier transform infrared analysis of fly ash geopolymer gel aging. Langmuir. 2007;23(16):8170–9. doi:10.1021/la700713g.
35. Miao X, Yimiao N, Shuxian L, Ling W, Long W, Sen W. Synthesis and structural characterization of fly ash based mineral polymer precursors. Front Mater. 2022;9. doi:10.3389/fmats.2022.837395.
36. Davidovits J. Geopolymers. J Therm Anal. 1991;37:1633–56. doi:10.1007/BF01912193.
37. Wu X, Shao G, Shen X, Cui S, Wang L. Novel Al2O3–SiO2 composite aerogels with high specific surface area at elevated temperatures with different alumina/silica molar ratios prepared by a non-alkoxide sol–gel method. RSC Adv. 2016;6:5611–20. doi:10.1039/c5ra19764c.
38. Patil GV, Joshi RS, Kazi RS, Kulsange SE, Kulkarni MJ. A possible role of glycation in the regulation of amyloid beta precursor protein processing leading to amyloid beta accumulation. Med Hypotheses. 2020;142:109799. doi:10.1016/j.mehy.2020.109799.
39. Duan Y, Wang P, Yang K. Study on hydration and hardening mechanism of alkali activated metakaolin cementitious materials. J New Build Mater. 2006;1:22–5.
40. Liu J, Zhang Y. Experimental study of fly ash geopolymer mortar. J Compr Utilization Fly Ash. 2018;2:46–9.
41. Wan X, Zhang Y, Zhao T. Mechanical properties of alkali activated slag concrete. J Mater Res. 2008;32:2091.
42. Liu G, Zhou B, Ni X, Shen J, Wu G, Du A, Zu G. Influence of thermal process on microstructural and physical properties of ambient pressure dried hydrophobic silica aerogel monoliths. J Sol-Gel Sci Technol. 2012;62(1):126–33. doi:10.1007/s10971-012-2694-x.
43. Guo Y. Preparation and properties of Al2O3 aerogels and composites. Guangzhou: South China University of Technology; 2016.

